ASTRONOMY & ASTROPHYSICS
SUPPLEMENT SERIES

Astron. Astrophys. Suppl. Ser. **139**, 625–628 (1999)

Hyperfine population measurement of excited OH from H_2O photodissociation by microwave stimulation – first results

T. Thissen[1], **H. Wurps**[1], **H. Spiecker**[1], **J.J. ter Meulen**[2], **and P. Andresen**[1]

[1] Angewandte Laserphysik, University of Bielefeld, Universitaetsstr. 25, D-33615 Bielefeld, Germany
[2] Department of Molecular and Laser Physics, University Nijmegen, Toernooiveld 1, NL-6525 ED Nijmegen, The Netherlands

Received February 17; accepted July 22, 1999

Abstract. In this paper the first measurement of the hyperfine population of a photofragment is presented. The population of the hyperfine levels of the $^2\Pi_{3/2}(J = 7/2)$ state of OH out of photodissociation of cold H_2O turns out to be statistical. After photodissociation of water at 157 nm within a Fabry-Perot microwave cavity the nascent OH formed in the $v = 0$, $J = 7/2$ state (probed by LIF) is stimulated by microwave radiation. From saturation data the population in each hyperfine level in both Λ-doublets is determined.

Key words: masers — molecular data — ISM: molecules — radio lines: ISM

1. Introduction

The pump mechanism of OH masers in star forming regions (e.g. W3(OH)) has been a field of intensive research in the last decade. There are several rival models for this pump mechanisms under discussion (Andresen 1985; Piehler & Kegel 1989; Cesaroni & Walmsley 1991; Gray et al. 1992; Elitzur 1996). A proper understanding of these masers would deliver detailed information about the physical conditions in these regions, e.g. grain temperature and grain density, magnetic fields, OH and H_2O densities, radiation fields (Reid 1993; Gray & Field 1995; Pavlakis & Kylafis 1996; Thissen et al. 1999). OH masers could then be used as a diagnostics tool for regions of star formation.

We assume that photodissociation of H_2O in the first absorption band ($135 - 190$ nm) plays a central role in the pumping mechanism for OH masers (Andresen et al. 1985; Thissen et al. 1999).

Send offprint requests to: T. Thissen
e-mail: tthissen@physik.uni-bielefeld.de
Correspondence to: Angewandte Laserphysik, University of Bielefeld, Universitaetsstr. 25, 33615 Bielefeld, Germany.

This work is one step in a series of laboratory experiments to measure the nascent OH population out of photodissociation of H_2O. It was shown by Andresen et al. 1985 that photodissociation of rotationally cold H_2O at 157 nm leads to a population inversion between the Λ-doublets of the OH-fragment. Wurps et al. (1996) reported a population inversion between the Λ-doublets for the OH $^2\Pi_{3/2}(J = 7/2)$ state of 1.8:1. Wurps measured the changing of the Λ-doublet population for the OH $^2\Pi_{3/2}(J = 7/2)$ state by microwave stimulation. Linebroadening mechanisms for the hyperfine transitions were understood quantitatively.

This paper deals with the question whether photodissociation of H_2O yields a non statistic population of the hyperfine levels of each Λ-doublet to explain satellite line maser emission. However, a statistical population is found within the error limits of the experiment.

2. Experimental method

The experimental set-up is already described in detail in Wurps et al. (1996).

A heated General Valve pulsed nozzle is used to produce a molecular beam of rotationally cold water which is directed between the plates of a Fabry-Perot microwave cavity. The Fabry-Perot cavity is part of a microwave system that can be tuned to the resonance frequency of the OH $^2\Pi_{3/2}(J = 7/2)$ Λ-doublet transitions $F \rightarrow F'$ around 13.4 GHz. The microwaves are produced by a frequency stabilised klystron and are amplified with an HP 83006A microwave amplifier up to a maximum output of +13 dBm.

A part of the H_2O molecules are dissociated by a F_2 excimerlaser in the center of the microwave cavity. The OH fragments are subsequently detected by LIF with an excimer pumped frequency doubled dye laser via the OH ($^2\Sigma - ^2\Pi$) absorption band around 308 nm. The dye laser

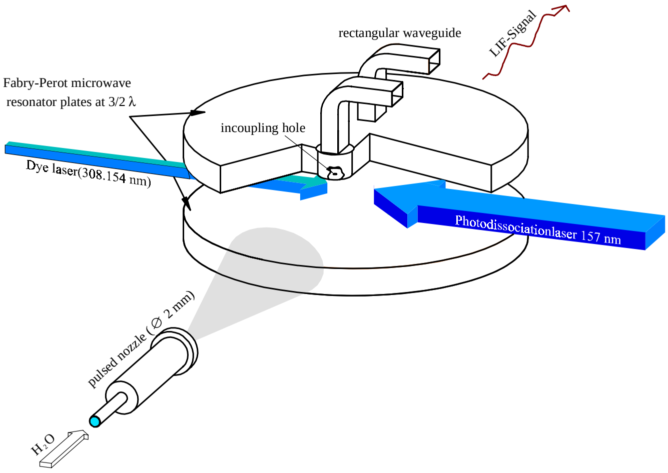

Fig. 1. Overview over the experimental set-up. The reaction volume is in the centre of the microwave Fabry-Perot cavity. The H_2O molecular beam is generated by a pulsed General Valve nozzle. The H_2O molecules are dissociated by a F_2 excimer laser at 157 nm. The OH fragments are detected by LIF via the $Q_1(3)$ line

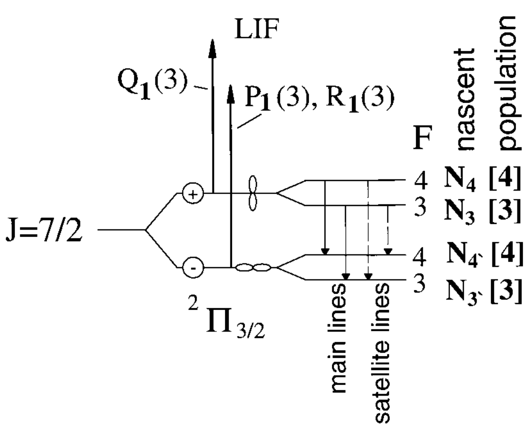

Fig. 2. The schematic energy level diagram shows the $^2\Pi_{3/2}(J = 7/2)$ state in OH. The arrows indicate the induced microwave transitions and the LIF transitions

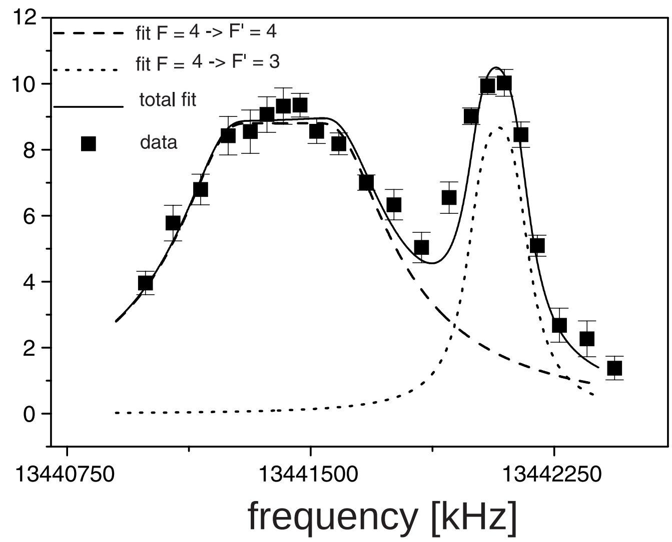

Fig. 3. Population change of the $^2\Pi_{3/2}(J = 7/2,\ A')$ state under interaction with microwaves in the vicinity of the $F = 4 \rightarrow F = 4'$ and the $F = 4 \rightarrow F = 3'$ transition detected with LIF via $Q_1(3)$

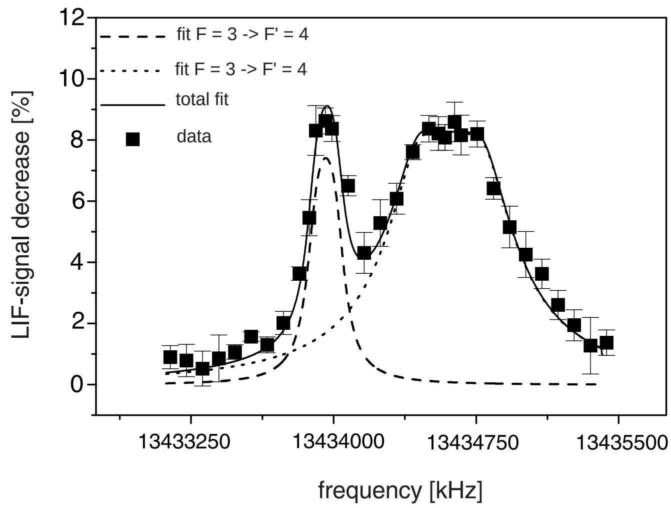

Fig. 4. Population change of the $^2\Pi_{3/2}(J = 7/2, A')$ state under interaction with microwaves in the vicinity of the $F = 3 \rightarrow F = 3'$ and the $F = 3 \rightarrow F = 4'$ transition detected with LIF via $Q_1(3)$

is tuned to the $Q_1(3)$ line detecting the upper Λ-doublet of the $^2\Pi_{3/2}(J = 7/2)$ state. The LIF signal is imaged onto an intensified CCD-camera and typically averaged over 100 laser shots.

The relative microwave induced population change between the Λ-doublets results in a change of the LIF signal. The relative population change was measured for the main lines ($\Delta F = 0$) and the satellite lines ($\Delta F = 1$). Figure 2 shows a level diagram of the hyperfine structure for the OH $^2\Pi_{3/2}(J = 7/2)$ state with the induced microwave transitions and the LIF detection.

3. Results

The relative population change of the LIF signal was measured as a function of the stimulating microwave frequency. Figure 3 shows the $F = 4 \rightarrow F' = 4$ line together with the $F = 4 \rightarrow F' = 3$ line. Figure 4 shows the $F = 3 \rightarrow F' = 3$ line together with the $F = 3 \rightarrow F' = 4$ line. The incoupled microwave power was +6.5 dBm which leads to saturation in the main lines and in the satellite lines. The interaction time between the OH molecules and the microwave field is given by the delay between the OH production by the VUV-laser and the detection by the

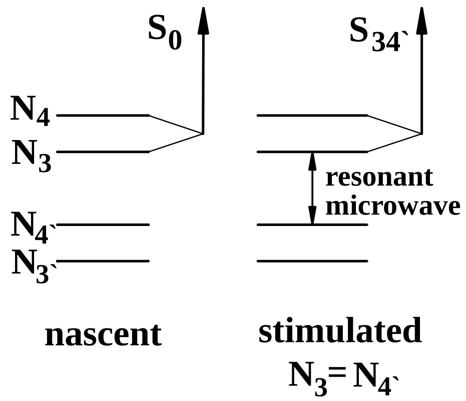

Fig. 5. Schematic diagram of the two experimental cases in our experiment. The nascent LIF signal S_0 is proportional to the population of the upper Λ-doublet. In the second case the microwave radiation couples two hyperfine levels (e.g. $F = 3 \rightarrow F = 4'$ transition). If the microwave transition is saturated in our experiment,thus the population of each magnetic state $(N_F, N_{F'})$ of the two coupled hyperfine states is equalised. The change in the LIF signal can be measured. The relative LIF signal change is related to the nascent population of the hyperfine levels

LIF excitation which terminates the interaction relevant for the results. The interaction time was 10 μs. Because of the higher dipole transition moment the main lines show a stronger saturation broadening than the satellite lines. The fitting includes saturation broadening, Doppler broadening and lifetime broadening (Wurps et al. 1996).

Population distribution of the hyperfine states

The LIF excitation does not resolve the hyperfine splitting of the Λ-doublet states. Nevertheless it is possible to calculate the population be the relative population change between th Λ-doublets. Thus the observable which is dealt with is the relative population change of the upper Λ-doublet in case of an interaction of the ensemble of OH fragments with microwave radiation of the $F \rightarrow F'$ transition ($P_{FF'}$). The measured $P_{FF'}$ are shown in Table 1. The $P_{FF'}$ are given by

$$P_{FF'} = \frac{S_0 - S_{FF'}}{S_0} \tag{1}$$

with S_0 = LIF intensity of the $Q_1(3)$ line without microwave stimulation and $S_{FF'}$ = LIF intensity of the $Q_1(3)$ after microwave stimulation. The LIF transistion is saturated. Thus the LIF intensity is proportional to the population of the Λ-doublets. Figure 5 shows the two experimental cases for the $F = 3 \rightarrow F = 4'$ transition. In the first case the LIF signal S_0 is proportional to the nascent population of the upper Λ-doublet

$$S_0 = c \cdot (N_4[4] + N_3[3]) \tag{2}$$

with N_F being the population of each magnetic state of the hyperfine levels, $[x] = 2x + 1$ the multiplicity of each hyperfine level and c a constant factor. In the case of saturated microwave stimulation the population of the magnetic states of the two coupled hyperfine levels are equalised. In our example the N_3 is equal $N_{4'}$. The population of the upper $F = 3$ hyperfine level after stimulation (N_3^{stim}) is then given by

$$N_3^{\text{stim}} = \frac{N_3[3] + N_{4'}[4']}{[3] + [4']}. \tag{3}$$

The LIF signal $S_{34'}$ is

$$S_{34'} = c \times \left(N_4[4] + N_3^{\text{stim}}[3]\right) \tag{4}$$

$$= c \times \left(N_4[4] + \frac{N_3[3] + N_{4'}[4']}{[3] + [4']}[3]\right). \tag{5}$$

This leads to four linear equations one for each microwave transition:

$$S_{4F'} = c \times \left(\frac{N_4[4] + N_{F'}[F']}{[4] + [F']}[4] + N_3[3]\right) \tag{6}$$

$$S_{3F'} = c \times \left(\frac{N_3[3] + N_{F'}[F']}{[3] + [F']}[3] + N_4[4]\right) \tag{7}$$

with $F' = 4$ or $F' = 3$. Equations (2), (6), (7) put in Eq. (1) gives a system of four linear equations which connects the observable $P_{FF'}$ to the population of the hyperfine levels:

$$P_{FF'} = \frac{[F][F']}{[F] + [F']} \frac{(N_F - N_{F'})}{N_4[4] + N_3[3]}. \tag{8}$$

The solution of the equation system for the values of $P_{FF'}$ in Table 1 is shown in Table 2. The measured distribution of the hyperfine levels corresponds to a statistical distribution of $[F]/([4] + [3])$ per hyperfine level for each Λ-doublet.

Table 1. Fitting parameters for Fig. 3 and Fig. 4. The resonance frequency, the FWHM and the $P_{FF'}$ are taken from the figures. The dipole moment is taken from Destombes et al. (1977). The main lines with $\Delta F = 0$ show a stronger saturation broadening than the satellite lines with $\Delta F = 1$

Transition $F \rightarrow F'$	Resonance frequency [GHz]	Dipole moment 10^{-30}[cm]	FWHM [kHz]	$P_{FF'}$ [%]
$4 \rightarrow 4$	13.441417	1.91	770	8.8 ± 0.52
$4 \rightarrow 3$	13.442076	0.3661	206	8.7 ± 0.36
$3 \rightarrow 3$	13.434637	1.91	766	8.2 ± 0.34
$3 \rightarrow 4$	13.434001	0.3229	188	7.4 ± 0.55

4. Conclusion

The population distribution of the hyperfine levels in the OH $^2\Pi_{3/2}(J = 7/2)$ state is determined. The measured distribution corresponds well to a statistical form. With this result, the nascent population of the hyperfine levels

Table 2. Measured population of the hyperfine levels in the $^2\Pi_{3/2}(J = 7/2)$ state of OH out of the photodissociation of water. The measured distribution corresponds well with the statistical distribution

Λ-doublet	hyperfine level F	measured distribution [%] $N_F[F]$	statistical distribution[%] $\frac{[F]}{[4]+[3]}$
upper	$F = 4$	56.2 ± 1.14	56.25
	$F = 3$	43.8 ± 0.86	43.75
lower	$F = 4$	58.3 ± 1.19	56.25
	$F = 3$	41.7 ± 0.82	43.75

of OH out of photodissociation of H_2O is determind and can be used for astrophysical models (e.g. Thissen et al. 1999). The statistical population distribution and the much smaller dipole transition moment (see Table 1) rules out maser emission on the satellite lines in the OH $^2\Pi_{3/2}(J = 7/2)$ state. In fact the satellite lines of this state are not observed in emission or in absorption (Matthews et al. 1986; Baudry & Diamond 1998).

In contrast to this the OH ground state shows laser emission on the satellite line. Secondary processes (e.g. IR relaxation from excited OH or IR pumping) has to be taken into account to explain these maser actions.

Acknowledgements. This work was supported by the Sonderforschungsbereich 216 der Deutschen Forschungsgemeinschaft. We also thank the department of Molecular and Laser Physics of the University Nijmegen for the free disposal of the microwave system.

References

Andresen P., 1985, A&A 154, 42
Baudry A., Diamond P.J., 1998, A&A 331, 697
Cesaroni R., Walmsley C.M., 1991, A&A 241, 537
Destombes J.L., Marliere C., Baudry A., Brillet J., 1977, A&A 60, 55
Elitzur M., 1996, ApJ 457, 415
Gray M.D., Field D., 1995, A&A 298, 243
Gray M.D., Field D., Doel R.C., 1992, A&A 262, 555
Gray M.D., Field D., 1995, A&A 298, 243
Matthews H.E., Baudry A., Guilloteau S., Winnberg A., 1986, A&A 163, 177
Pavlakis K.G., Kylafis N.D., 1996, ApJ 467, 309
Piehler G., Kegel W.H., 1989, A&A 214, 339
Reid M.J., 1993, BAAS 182, 26.05
Schinke R., Engels V., Andresen P., Balint-Kurti G.G., 1985, Phys. Rev. Lett. 51, 386
Thissen T., Spiecker H., Andresen P., 1999, A&AS 133, 323
Wurps H., Spiecker H., ter Meulen J.J., Andresen P., 1996, J. Chem. Phys. 105, 2654